Rail Vehicle Model Dynamics of Motion Along Straight Track with Vertical Irregularity

Mirosław DUSZA[1]

Summary
During the long-term exploitation of railway tracks, possible changes in ground conditions may result in downgrading the quality of the drainage systems. The lack of adequate drainage of the track substructure leads to a lowering of the track formation cohesion ensured during the track construction phase as a result of ballast tamping. This potentially leads to pushing ballast into the subsoil, affecting the ballast which is present directly below the sleepers loaded during passage of the vehicles. As a result, the sleepers are no longer supported by ballast. The loss of support may affect a single sleeper or a set of neighbouring sleepers, depending of the length of the zone with inadequate drainage. Rail vehicle runs over such zones cause track vertical irregularities. This article is devoted to analysis of the influence of such irregularities on the rail vehicle dynamics. An arrangement model comprising a passenger coach and ballasted track was created with the VI-Rail tool. Coach runs were simulated within the range of operational speeds. Attention was paid to observation of the wheel-rail contact forces, which appeared during runs over different lengths of vertical irregularities. The obtained results are compared with currently binding criteria and regulations.

Keywords: rail vehicle dynamics, track irregularities, wheel-rail contact forces, numerical simulation

1. Introduction

The long-term exploitation of railway tracks causes gradual downgrading, which is sometimes significantly different on neighbouring pieces of track. This is a complex process affected by many factors. Subsoil properties which may change over long-term track exploitation belong to such factors. Track wear results in irregularities with different values and different directions. Irregularities grow with time and the transported mass of goods and directly influence the dynamics of the vehicle-track interaction [8]. Generally, track irregularities are subdivided into vertical and lateral direction [1, 13]. Within the research works presented below, the influences of vertical irregularities only were analysed. The appearance and increase of such irregularities is caused, among others, by non-uniform track lowering usually caused by adverse subsoil properties. (e.g. limited rain water passage). Usually, in such cases, the deflection of one or both rails takes place, over the distance of three or more neighbouring sleepers. The so-called "mud outflow" is the final stage of such damage, indicating the loss of support for part of or the whole sleeper (see Figure 1).

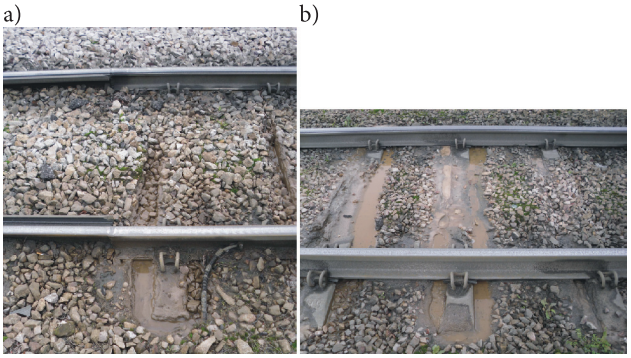

Fig. 1. Lack of sleeper vertical support: a) under one rail, b) under the whole length of a sleeper [photo. M. Dusza]

Track deflection initiated on a single sleeper causes an increase in the forces with which wheelsets act on neighbouring sleepers. As a result, both the lowering of those sleepers and length of the track irregularity zone grow when wheelsets pass. The consequences of such damage lead directly to permanent track deformations and create a real vehicle derailment risk [2, 12, 15].

[1] Ph.D., D.Sc. Eng.; Warsaw University of Technology, Faculty of Transport; e-mail: mdusza@wt.pw.

2. Aim and range of research

Dynamic vehicle-track interactions due to running over a single longitudinal irregularity caused by a lack of support for, respectively: one, two and three neighbouring sleepers under one rail were tested (see Figure 2). Each passing vehicle wheelset causes (right) rail vertical deflection and the appearance of track twist [1, 13]. Assuming a typical arrangement of sleepers in a track of 0.65 m [1, 13, 14], depending on the number of sleepers without ballast support, the obtained length of the wave of longitudinal irregularity may be equal to:
L = 2.6 m – for one unsupported sleeper,
L = 3.9 m – for two unsupported sleepers,
L = 5.2 m – for three unsupported sleepers.

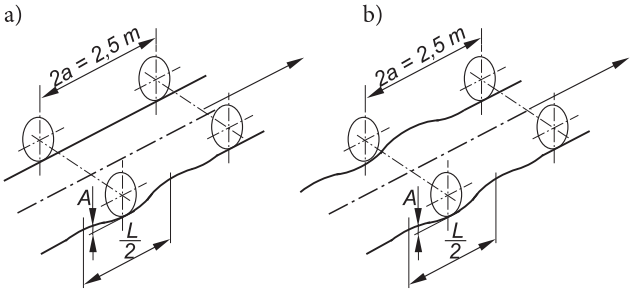

Fig. 2. Vertical irregularity: a) on the right rail, b) on both rails [own elaboration]

The rail deflection amplitude A depends, among others, on the vertical load caused by wheelsets. For the tests which are presented in this article, a constant value of A = 0.01 m was assumed. An irregularity is interpolated in simulations by half of sine wave with a period and amplitude respective to the values L and A given above. The distance between wheelsets in a bogie of the coach in the model equals $2a$ = 2.5 m. Therefore, for each L value, a run over the irregularity causes track twist and creates a hazard of abrupt change in the values of wheel-rail contact forces [9].

Moreover, this also causes a derailment risk, especially for vehicles with high wheelset guiding rigidity (e.g. for cargo wagons) [15]. The chosen parameters of the vehicle-track interaction were tested (in the article, wheel-rail forces) for vehicle runs with speeds from 5 to 60 m/s on a straight track with a vertical irregularity representing the loss of support under, respectively, one, two and three sleepers (see Figure 3). The first stage of the tests reflects the loss of sleeper support under one rail (right rail – see Figure 2). The second stage reflects the symmetrical loss of support under both rails. The track is assumed to have no other irregularities. The critical velocity for the tested vehicle in the model equals v_n = 61.7 m/s [3–6]. Therefore, running over the irregularity is the only cause of the observed changes in parameters (there are no conditions favourable e.g. for self-excited vibrations appearance) [16, 18].

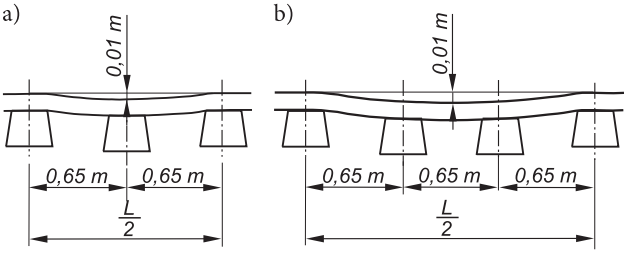

Fig. 3. Vertical irregularity as an effect of loss of support by: a) one sleeper, b) two neighbouring sleepers [own elaboration]

3. Tested model

The model was created with the VI-Rail engineering software. This is a discrete model of a type 127A passenger coach (see Figure 4). Bogie models are based on a 25AN construction. The complete coach model is composed of 15 rigid bodies: coach body, two bogie frames, four wheelsets and eight axle-boxes. Rigid bodies are connected with elastic-dumping elements having linear and bi-linear characteristics.

The coach model is complemented by vertically and laterally flexible track model reflecting parameters corresponding to European ballasted track. Nominal profiles of S1002 wheels and UIC60 rails with the inclination 1:40 were used. The non-linear contact parameters are calculated with the ArgeCare RSGEO software. For calculating static wheel-rail contact forces, simplified Kalker theory is used and implemented as the FASTSIM procedure [8]. Motion equations are solved with use of the Gear procedure. A more detailed description of the model can be found in [4–6 and 16].

4. Test results

4.1. Lack of sleeper support under a single rail

Wheel-rail contact forces are particularly important for running safety. Changes in those forces were observed for the first wheelset on the right rail. The results of a run simulation with a velocity of 20 m/s are shown in Figure 5. In this case, the track has an irregularity corresponding to two unsupported sleepers (L = 3.9 m). From each simulation, the minimum value (*min*) and maximum value (*max*) of the vertical force Q and lateral force Y are read.

In the tested model, the constant value Q_{stat} is determined by the static vertical load for each wheel and

equals 55 390 N [4]. While the coach running velocity is being increased, the maximum values increase and minimum values decrease for vertical forces. Correlating the read results obtained for running speeds in a range of coach movement 5...60 m/s resulted in preparation of the graphs shown in Figure 6.

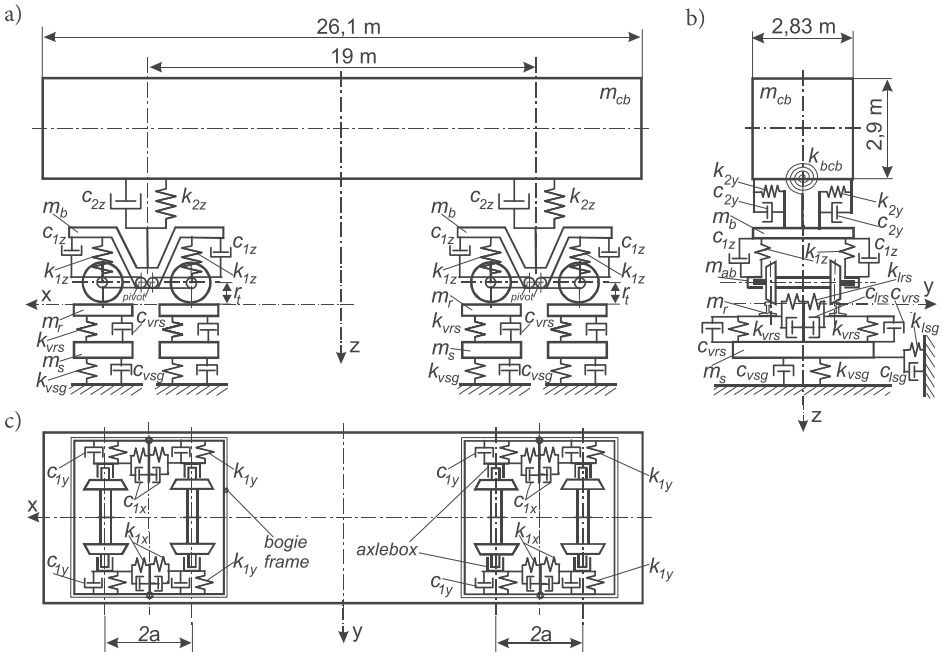

Fig. 4. Tested model diagram: a) side view, b) front view, c) top view [own elaboration]

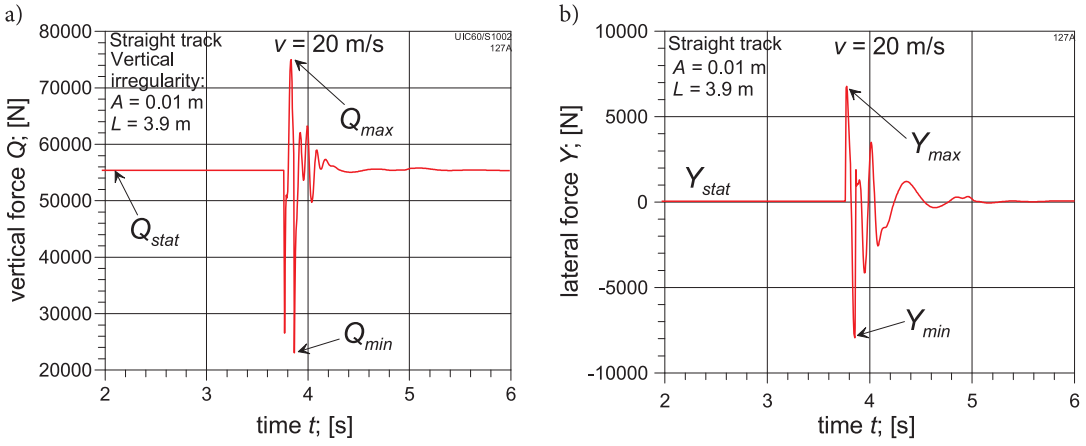

Fig. 5. Wheel-rail contact forces: a) vertical, b) lateral; for the first wheelset on the right rail while passing the vertical irregularity with the amplitude A = 0.01 m and wave length L = 3.9 m with the velocity of v = 20 m/s [own elaboration]

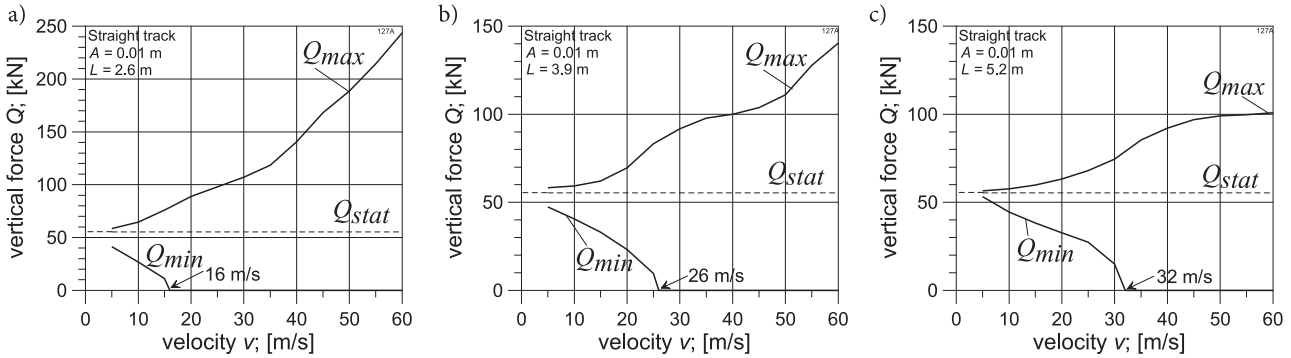

Fig. 6. Minimum and maximum values of the vertical wheel-rail contact forces Q on the right rail for the first wheelset passing irregularity with the wave length L: a) 2.6 m, b) 3.9 m, c) 5.2 m [own elaboration]

It can be seen that there is a characteristic running velocity, depending on the wave length of the irregularity, for which the minimum value of the vertical force Q_{min} reaches zero. This value increases with an increase in the length of the irregularity and equals: for L = 2.6 m – 16 m/s, for L = 3.9 m – 26 m/s, and for L = 5.2 m – 32 m/s. In theoretical considerations, this means a temporary increase in the value of the derailment safety coefficient Y/Q up to extremely high values (theoretically up to ∞) [12, 15]. In reality, this can mean a temporary loss of wheel-rail contact which creates a derailment hazard. The maximum values of the vertical contact force also depend on the length of the irregularity. The highest values occur for the shortest irregularity L = 2.6 m and reach about 240 kN, while for L = 3.9 m they reach about 140 kN. The lowest values occur for L = 5.2 m and reach about 100 kN.

The lateral wheel-rail contact forces Y change their values and direction. From the point of view of impact on the track, the Y force direction for the straight track is insignificant. In order to easily compare the values Y_{min} with Y_{max} in Figure 7, the presented values are absolute values $|Y_{min}|$. The highest Y values occur for passing the irregularity with the wave length L = 2.6 m and reach about 40 kN. For L = 3.9 m they are slightly lower and for L = 5.2 m significantly lower and reach about 12 kN.

According to the standard [7], the limit of permissible values for the track impacting vertical forces $Q_{max,lim}$ depend on the maximum permissible vehicle velocity which is reached on the analysed track section v_{adm} and can reach:
$Q_{max,lim}$ = 200 kN – for $v_{adm} \leq$ 160 km/h (about 44.44 m/s);
$Q_{max,lim}$ = 160 kN – for v_{adm} > 300 km/h (about 83.33 m/s).

For each tested irregularity wave length, the vertical forces impacting the track increase together with increased velocity. Only for the shortest irregularity wave, do they reach and exceed permissible values (see Figure 8*a*). For the velocity of about 52 m/s (about 187.2 km/h) the highest permissible value $Q_{max,lim}$ = 200 kN is exceeded. This is not an issue, as permissible velocity then equals $v_{adm} \leq$ 160 km/h. However, for the velocity of about 44 m/s (about 158.4 km/h) $Q_{max,lim}$ = 160 kN is exceeded, which is permissible on track sections with the maximum allowed velocity v_{adm} > 300 km/h. The appearance of such an irregularity therefore creates a substantial constraint for making use of high velocity running possibilities on routes adjusted for such velocities (High Speed Railways). For the higher irregularity

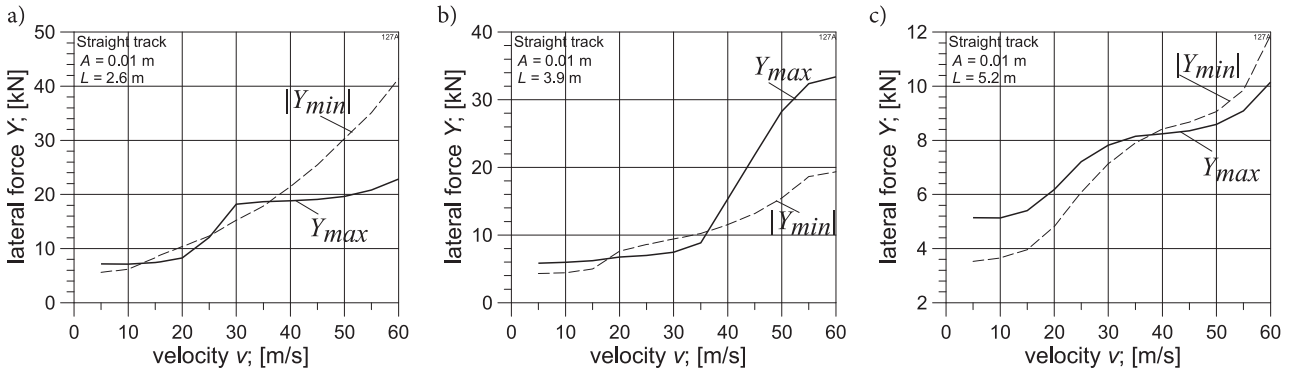

Fig. 7. Minimum and maximum values of the lateral wheel-rail contact forces on the right rail for the first wheelset passing irregularity with the wave length L: a) 2.6 m, b) 3.9 m, c) 5.2 m [own elaboration]

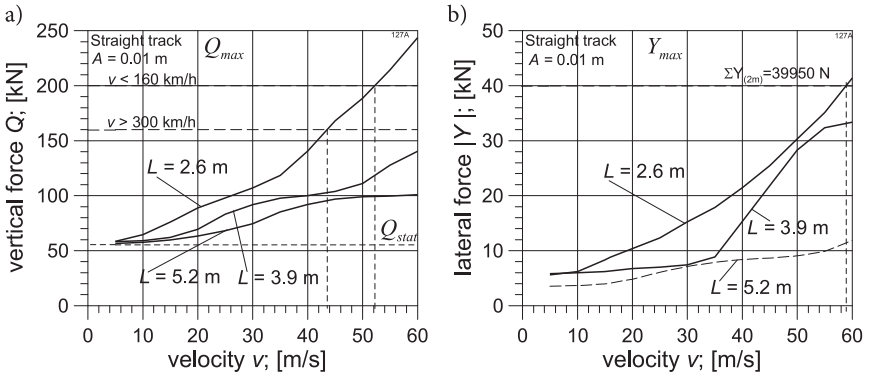

Fig. 8. Maximum values of the vertical (a) and lateral (b) wheel-rail contact forces for the first wheelset on the right rail while passing irregularities with the wave lengths L = 2.6 m, 3.9 m and 5.2 m [own elaboration]

wave lengths (L = 3.9 and 5.2 m) within the tested range of velocities 0...60 m/s, vertical forces do not exceed the minimum permissible value $Q_{max\,lim}$ = 160 kN.

Extreme absolute values of the lateral forces with which the wheel passing the irregularity impacts on the track $|Y|$ are correlated in Figure 8b. Those forces increase with increased velocity. The permissible value of the lateral force acting on the track for the tested vehicle-track model was defined in earlier tests [4] on the basis of the Prud'homme criterion. The value of this force has been estimated to be $\Sigma Y_{(2m)}$ = 39 950 N. Respecting this value ensures the maintenance of rail and sleeper positioning in relation to the track ballast. It can be spotted that only for the shortest wave irregularity L = 2.6 m is the permissible value exceeded for velocity higher than 59 m/s (212,4km/h). For two other lengths of the wave irregularities L, the forces $|Y|$ fit in the range of permissible values.

4.2. Lack of support under the whole length of sleepers

The second analysed case reflects the loss of support under the whole length of sleepers (see Figures 1b and 9). In the tests presented, it has been modelled as a symmetrical longitudinal irregularity on both rails with parameters analogical to those used for the previously tested case (the same lengths of waves and amplitude 0.01 m). The observed parameters are wheel-rail contact forces for the first wheelset on the right rail.

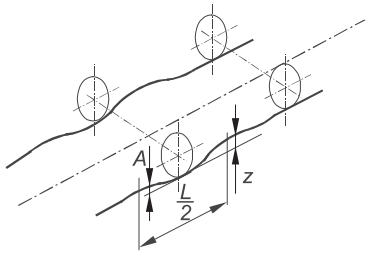

Fig. 9. Symmetrical vertical irregularity on both rails [own elaboration]

It can be observed that the character of variations of the vertical force values Q, in the running velocity domain, is similar to the previously tested case, although the values are significantly bigger (see Figure 10). The maximum values Q_{max} increase together with increased velocity for each track irregularity. The maximum $Q_{max} \approx$ 390 kN occurs for L = 2.6 m. For L = 3.9 m Q_{max} reaches 290 kN and for L = 5.2 m $Q_{max} \approx$ 195 kN. These values are, therefore, nearly two times bigger than those observed while passing over an irregularity under one rail. The minimum Q values decrease together with increased velocity. As in the previously tested case, there are characteristic running velocities for which Q_{min} = 0. They are, however, smaller than those occurring in the previous case and equal: 13 m/s for L = 2.6 m (previously 16 m/s), 21 m/s for L = 3.9 m (previously 26 m/s) and 23 m/s for L = 5.2 m (previously 32 m/s). In reality, this can mean that for a symmetrical double-rail vertical irregularity the loss of wheel-rail contact takes place for lower running velocity.

Extreme values of the lateral contact forces Y increase with increased velocity (see Figure 11). As previously, movement takes place on a straight track and therefore the Y force direction is insignificant. On the graphs, the negative values of Y_{min} are shown as $|Y_{min}|$.

It can be seen, while comparing the extreme Y values for both tested cases (see Figures 7 and 11), that for a symmetrical double-rail irregularity the Y values are significantly smaller. For the irregularity wave length L = 2.6 m lateral forces reach about 11.5 kN (previously about 40 kN), for L = 3.9 m about 8.2 kN (previously about 34 kN) and for L = 5.2 m about 4 kN (previously about 12 kN).

The obtained results of calculations are correlated in Figure 12. Relating to the binding standards and regulations [7, 14] show that the permissible values of the vertical forces are exceeded while passing the irregularity for each tested length. It is the earliest for L = 2.6 m as already for velocity about 28 m/s the force Q reaches values permissible on high speed

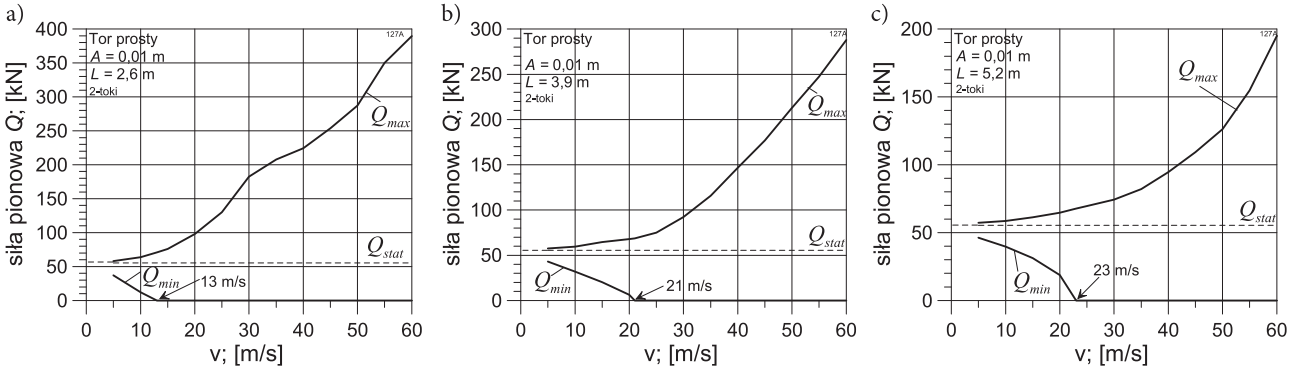

Fig. 10. Minimum and maximum values of the vertical wheel-rail contact forces on the right rail for the first wheelset passing a double-rail irregularity with the wave length L: a) 2.6 m, b) 3.9 m, c) 5.2 m [own elaboration]

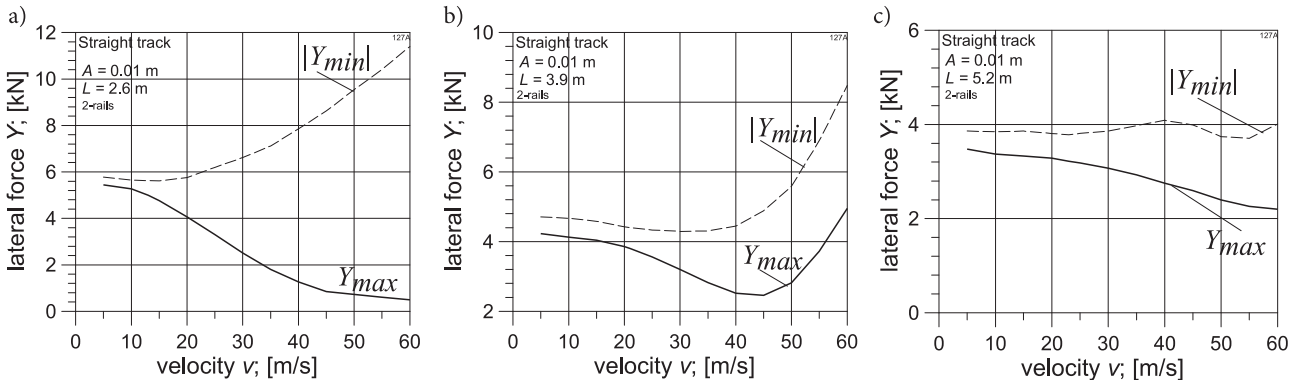

Fig. 11. Minimum and maximum values of the lateral wheel-rail contact forces on the right rail for the first wheelset passing a double-rail irregularity with the wave length L: a) 2.6 m, b) 3.9 m, c) 5.2 m [own elaboration]

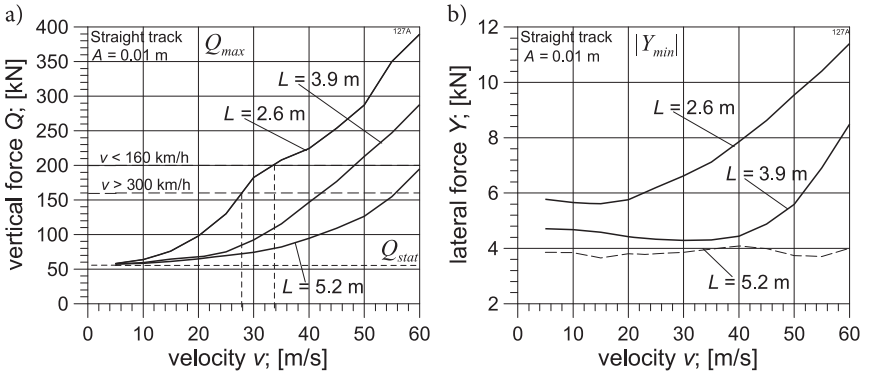

Fig. 12. Maximum values of the vertical (a) and lateral (b) wheel-rail contact forces for the first wheelset on the right rail while passing a vertical symmetric double-rail irregularity with the wave lengths L = 2.6 m, 3.9 m and 5.2 m [own elaboration]

routes and for velocity about 34 m/s on all routes. For L = 3.9 m the permissible Q values are reached for velocities about 42 and 48 m/s. For velocities above 55 m/s for the longest irregularity wave L = 5.2 m the force Q exceeds permissible values.

5. Conclusions

Railway routes pass sites on which proper subsoil dewatering is an important problem. Vertical irregularities may appear there as a result of insufficient drainage. The performed tests show that this can lead to an important increase in dynamic load in the case of tracks where one sleeper or more neighbouring sleepers have lost their vertical support as a result of the loss of subsoil elastic properties. Increased values of loads must be then taken by sleepers neighbouring the unsupported sleepers. This creates propitious conditions for the widening of zones with unsupported sleepers and further track degradation. The loss of sleeper support under one rail while the second rail is supported leads to the so-called track twist. Such an irregularity potentially leads to the temporary loss of wheel-rail contact and derailment, especially in the case of vehicles with high suspension rigidity on the first stage of suspension. Then, in the case of traction vehicles, traction capabilities are reduced or even lost (wheel sliding) leading to quicker wear of wheel and rail profiles [11]. Increased track load caused by the tested irregularity has a dynamic character. The maximum values of vertical and lateral forces grow together with increased vehicle running velocity. However, irregularity wave length also has an important influence on the maximum values of contact forces. The highest values appear for the shortest irregularities (one unsupported sleeper) and decrease together with increases in irregularity wave length. Perhaps such dependability arises from the preconceived constant value for the rail deflection amplitude for each tested irregularity length. In reality, it should be rather expected that deflection amplitude will grow with increased irregularity wave length (higher amount of unsupported sleepers) for defined loads from vehicles. Verifying whether such dependability exists requires further tests.

The time for vehicle wheel passage over the tested irregularities is counted in fractions of a second (see Figure 5). The observed effects of passage should therefore be recognized as fast-changing processes. As a result, explanation is needed regarding the resolution of the observed parameters. A step in tabulation of the results is a crucial parameter for the resolution of numerical calculations. For the tests shown, simulation

time was set to 15 seconds within which the calculation results were noted in 2500 tabulation rows. A step in tabulation is therefore 15/2500 = 0.006 s (time is an independent variable). This means that peak values (pulses) of the contact forces which last shorter than 0.006 s may be unidentified in tests.

Literature

1. Bałuch H.: *Diagnostyka nawierzchni kolejowej*, Wydawnictwa Komunikacji i Łączności, Warszawa 2003, s. 189.
2. Chudzikiewicz A., Sowiński B., Szulczyk A.: *Zagrożenie bezpieczeństwa ruchu pojazdów szynowych spowodowane stanem toru*, Problemy Eksploatacji, Maintenance Problems, 2009 nr 4, s. 177–192.
3. Dusza M., Zboiński K.: *Wybrane zagadnienia dokładnego wyznaczania wartości prędkości krytycznej modelu pojazdu szynowego*, Kwartalnik Pojazdy Szynowe, 1/2012, s. 13–19.
4. Dusza M.: *Stateczność ruchu układu pojazd szynowy – tor. Modelowanie, metoda, badania*, Oficyna Wydawnicza Politechniki Warszawskiej, Warszawa 2016, s. 1–143.
5. Dusza M.: *The study of track gauge influence on lateral stability of 4-axle rail vehicle model.* Archives of Transport, volume 30, issue2, Warsaw 2014, pp. 7–20.
6. Dusza M.: *The wheel-rail contact friction influence on high speed vehicle model stability*, Transport Problems, volume 10, issue 3, [online 2300-861X], pp. 73–86, Wydawnictwo Politechniki Śląskiej, Gliwice 2015.
7. EN 14363:2005: Kolejnictwo – Badania właściwości dynamicznych pojazdów szynowych przed dopuszczeniem do ruchu – Badanie właściwości biegowych i próby stacjonarne.
8. Iwnicki S. (editor): *Handbook of railway vehicle dynamics*. CRC Press Inc., 2006.
9. Jian Zhang and other: *A linear complementary method for the solution of vertical vehicle-track interaction*, Vehicle System Dynamics, Vol. 56, No. 2, 2018, pp. 281–296.
10. Kalker J.J.: *A fast algorithm for the simplified theory of rolling contact*, Vehicle System Dynamics 11, 1982, pp. 1–13.
11. Olofsson U. and others: *Tribology of the wheel-rail contact – aspects of wear, particle emission and adhesion*, Vehicle System Dynamics, Vol. 51, No. 7, July, 2013, pp. 1091–1120.
12. Sobaś M.: *Stan doskonalenia kryteriów bezpieczeństwa przed wykolejeniem pojazdów szynowych*, Pojazdy Szynowe nr 4, 2005, s. 1–13 i nr 2, 2006, s. 37–48.
13. Sysak J.: *Drogi Kolejowe*, Wydawnictwo Naukowe PWN, Warszawa 1986.
14. Towpik K.: *Infrastruktura drogi kolejowej, obciążenia i trwałość nawierzchni*, Wydawnictwo Instytutu Technologii Eksploatacji – PIB, Warszawa – Radom 2006.
15. Wilson N. and others: *Assessment of safety against derailment using simulations and vehicle acceptance test: a worldwide comparison of state-of-the-art assessment methods*, Vehicle System Dynamics, Vol. 49, No. 7, July 2011, pp. 1113–1157.
16. Zboiński K., Dusza M.: *Bifurcation analysis of 4-axle rail vehicle models in a curved track*, Nonlinear Dynamics, July 2017, Volume 89, Issue 2, DOI 10.1007/s11071-017-3489-y, pp. 863–885.
17. Zboiński K., Dusza M.: *Extended study of rail vehicle lateral stability in a curved track*. Vehicle System Dynamics, Vol. 49, No. 5, May 2011, pp. 789–810.
18. Zboiński K., Dusza M.: *Self-exciting vibrations and Hopf's bifurcation in non-linear stability analysis of rail vehicles in curved track*. European Journal of Mechanics, Part A/Solids, Vol. 29, No. 2, 2010, pp. 190–203.